LES ON PLUME DISPERSION IN STABLE TURBULENT BOUNDARY LAYER

Tetsuro Tamura
Department of Environmental Science and Technology,
Tokyo Institute of Technology
4259 Nagatsuta, Yokohama, 226-8502 Japan
tamura@depe.titech.ac.jp

Kenichi Ohta
Department of Environmental Science and Technology,
Tokyo Institute of Technology
4259 Nagatsuta, Yokohama, 226-8502 Japan

ABSTRACT

This study discusses the characteristics of a plume dispersion in various types of thermally stratified stable turbulent boundary layers. Large eddy simulations (LES) of incompressible turbulent flows with the buoyancy effects based on the Boussinesq approximation are carried out for simulating atmospheric turbulent boundary layers. Concentration field inside a turbulent boundary layer, where gas is released from an elevated source point, is also obtained by using LES concept for a passive scalar. Dynamic procedure is used for estimation of Smagorinsky type of eddy viscosity model representing the sub-grid scale turbulent motions. LES results are validated by comparing with the previous experimental data or plotting plume spreading width in the Pasquill-Gifford diagrams. For modelling of stable boundary layers, we consider two kinds of temperature profiles whose inversion layers locate at the different heights according to the atmospheric stability or nocturnal time. Concentration fluctuations, especially peak values of concentration is focussed on, so we estimate a fitting of the computed time-sequential data with various probability distribution functions of concentration and statistically clarify the occurrence of peak concentration.

INTRODUCTION

For the environmental assessment to an impact of exhaust gases on people, the time-averaged value of their concentrations has been usually used in the past. In the case of flammable gas or noxious fume, however, it is important to clarify a state of high concentration that is mainly brought about by turbulence characteristics in the atmospheric boundary layer. Concerning the safety measures for diffusion of such hazardous gases, we have to appropriately estimate the peak value of concentration fluctuations. So, the time-dependent numerical model is strongly expected, in order to directly obtain a time variation of concentration without any statistical assumptions. In our past research, we performed Large Eddy Simulation (LES) of spatially-developing turbulent boundary layer and predicted the properties of the concentration field under the neutral condition for thermal stability(Tamura et al., 2003). Sykes and Henn(1992) also carried out LES of concentration fluctuations in a dispersing plume and compare the computed results with the previous experimental data. Henn and Sykes(1992) and Mason(1992) extend the LES technique to dispersion in the convective boundary layer. Turbulence structure and transport process in thermally stratified turbulent boundary layers, which can be generally seen in the actual atmospheric boundary layer, are much influenced and take on a complicated aspect because the effect of buoyancy drastically changes their flow fields as a basic property (Armerio and Sarkar, 2002, Tamura and Mori, 2006). Especially for establishment of safety against hazardous gases, the effect of thermal stratification on concentration fluctuations should be significantly examined. But almost researches have dealt with the case of unstable convective boundary layer and the stable case is very rare. In this research, we carry out LES analysis of dispersion in spatially-developing thermally stratified turbulent boundary layers, focusing on the stable case. Additionally, we set up the driver region where Lund's method(Lund et al., 1998) is applied for the generation of inflow turbulence. We employ the dynamic Smagorinsky model as subgrid-scale modeling of LES for flow and temperature fields. The objective of this research is mainly to investigate the dispersion characteristics of plumes emitted from an elevated source point in spatially-developing thermally stratified turbulent boundary layer, including concentration fluctuations and their peak values.

NUMERICAL MODEL FOR LARGE EDDY SIMULATION OF STABLE TBL

Figure 1 shows a numerical model for the simulation of thermally stratified boundary layers. In order to generate the inflow turbulence, in the driver region we used Lund's method that the turbulence parameters for velocity at recycle station are rescaled and introduced to the inlet boundary. The generated inflow data are imposed at entrance of the main computational region, and the temperature field begins to be solved in the main region introducing the buoyancy effect into the flow field. In this study, various types of temperature profiles are set at inflow

boundary of the main region. This process allows the generation of zero-pressure gradient spatially developing boundary layer with a small computational domain. We analyzed concentration field in the way to release passive scalar from an elevated source point at the main region.

The governing equations for LES consist of the filtered forms of the continuity equation, the momentum equation with a buoyancy term under the Boussinesq approximation, and the scalar (temperature and concentration) evolution equations for three-dimensional incompressible stratified flow as follows:

$$\frac{\partial \overline{u}_i}{\partial t} = 0 \tag{1}$$

$$\frac{\partial \overline{u}_i}{\partial t} + \overline{u}_j \frac{\partial \overline{u}_i}{\partial x} = -\frac{1}{\rho}\frac{\partial \overline{p}}{\partial x_i} + \frac{\partial}{\partial x_i}\frac{1}{\mathrm{Re}}\left(\frac{\partial \overline{u}_i}{\partial x_j} + \frac{\partial \overline{u}_j}{\partial x_i}\right) - \frac{\partial}{\partial x_i}\tau_{ij} + \beta g \overline{\theta}\delta_{i2} \tag{2}$$

$$\frac{\partial \overline{\theta}}{\partial t} + \overline{u}_j \frac{\partial \overline{\theta}}{\partial x_j} = \frac{\partial}{\partial x_j}\left(\frac{1}{\mathrm{Re}}\frac{1}{\mathrm{Pr}}\frac{\partial \overline{\theta}}{\partial x_j}\right) - \frac{\partial h_j}{\partial x_j} \tag{3}$$

$$\frac{\partial \overline{c}}{\partial t} + \overline{u}_j \frac{\partial \overline{c}}{\partial x_j} = \frac{\partial}{\partial x_j}\left(\frac{1}{\mathrm{Re}}\frac{1}{Sc}\frac{\partial \overline{c}}{\partial x_j}\right) - \frac{\partial s_j}{\partial x_j} \tag{4}$$

$$\tau_{ij} = \overline{u_i u_j} - \overline{u}_i \overline{u}_j \tag{5}$$

$$h_j = \overline{u_j \theta} - \overline{u}_j \overline{\theta} \tag{6}$$

$$s_j = \overline{u_j c} - \overline{u}_j \overline{c} \tag{7}$$

where u_i is the velocity, θ is the temperature, c is the concentration, t is the time, ρ is the density, p is the pressure, β is the thermal expansion coefficient and g is the gravity acceleration. Re is the Reynolds number, Pr is the Prandtl number and Sc is the Schmidt number as non-dimensional parameter. τ_{ij}, h_j and s_j are the subgrid-scale (SGS) Reynolds stress, heat flux and scalar flux, and represented by the eddy viscosity concept as follows:

$$\tau_{ij} - \frac{1}{3}\delta_{ij}\tau_{kk} = -2\nu_{SGS}\overline{S}_{ij} \quad , \quad \nu_{SGS} = C\overline{\Delta}^2\left|\overline{S}\right| \tag{8}$$

$$h_j = -\alpha_{SGS}\frac{\partial \overline{\theta}}{\partial x_j} \quad , \quad \alpha_{SGS} = \frac{\nu_{SGS}}{Pr_{SGS}} = C_\theta \overline{\Delta}^2\left|\overline{S}\right| \tag{9}$$

$$s_j = -\kappa_{SGS}\frac{\partial \overline{c}}{\partial x_j} \quad , \quad \kappa_{SGS} = \frac{\nu_{SGS}}{Sc_{SGS}} = \frac{C}{Sc_{SGS}}\overline{\Delta}^2\left|\overline{S}\right| \tag{10}$$

$$\overline{S}_{ij} = \frac{1}{2}\left(\frac{\partial \overline{u}_i}{\partial x_j} + \frac{\partial \overline{u}_j}{\partial x_i}\right) \quad , \quad \left|\overline{S}\right| = \sqrt{2\overline{S}_{ij}\overline{S}_{ij}}$$

We use the dynamic Smagorinsky model for SGS modelling of the momentum and the temperature equations. C and Cθ are individuually obtained by the dynamic procedure. For the concentration equation, however, the turbulent Schmidt number Sc_{sgs} is set to 0.5. The numerical method is based on a fractional-step method. For time marching of the momentum equation, the convection and diffusion terms are discretized respectively by the Adams-Bashforth and the Crank-Nicolson schemes. But for the temperature and the concentration equations, both terms are discretized by Adams-Bashforth scheme. All of the spatial derivatives are approximated by the second-order central difference. $\mathrm{Re}_\tau(=u_\tau\delta/\nu)$ and $\mathrm{Ri}_\tau(=g\beta\Delta\theta/u_\tau^2)$ are respectively 254 and 44 at inflow boundary, and changing in the streamwise direction for the case of the spatially-developing boundary layers.

Figure 2 displays the grid systems of driver and main regions for LES computations. Streamwise length is sufficient for representing a spatially-developing turbulent boundary layers. For the dispersion analysis gasses are emitted from an elevated point source at $0.2\delta_0$ in turbulent boundary layer. The main computational domain of $30\delta_0 \times 3.0\delta_0 \times 3.2\delta_0$, where δ_0 is boundary layer depth at inlet boundary, is resolved by $300 \times 45 \times 128$ grid points in the streamwise, vertical and horizontal directions(Table 1).

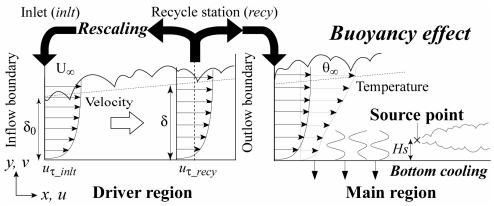

Figure 1: Numerical model for plume dispersion in stable turbulent boundary layer.

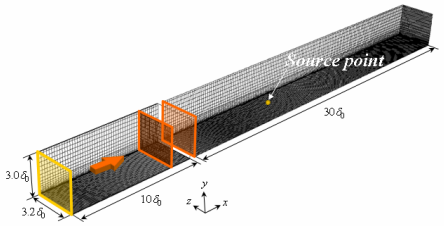

Figure 2: Grid systems of driver and main regions

Table 1: Computational conditions of main region

Grid	Region	Resolution
$x \times y \times z$	$30\delta_0 \times 3\delta_0 \times 3.2\delta_0$	$\Delta y^+_{max} = 33.7$
		$\Delta x^+ = 66$ $\quad$ $\Delta z^+ = 5.47$
$300 \times 45 \times 128$	$66 \times 6.6 \times 7.0$	$\Delta y^+_{min} = 0.636$

NUMERICAL VALIDATION FOR SPATIALLY DEVELOPING TURBULENT BOUNDARY LAYER

Here we validate a numerical model for the simulation of plume dispersion in the thermally stratified boundary layers. Neutral and stable boundary layers are separately discussed, comparing with the previous experimental data or the past scientific knowledge.

Neutral Boundary Layer

Figures 3 and 4 show the vertical profiles of mean velocity and turbulence statistics of neutral boundary layer. LES results and experimental data by Fackrell and Robins (1982) agree well each other.

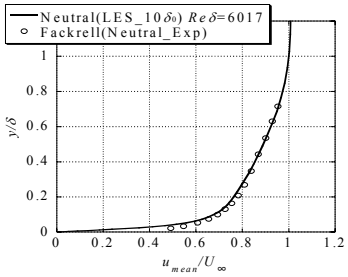

Figure 3: Mean velocity profile.

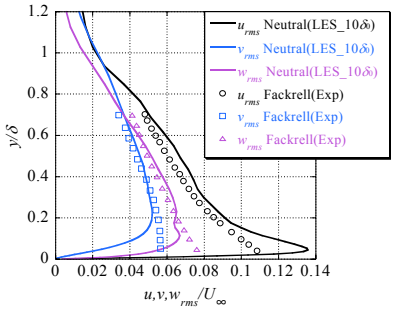

Figure 4: Turbulence statistics profile.

Time-averaged concentration. Figure 5 shows vertical profiles of time-averaged concentration for a plume dispersion emitted from an elevated point source in neutral turbulent boundary layer, compared with the wind tunnel experimental data under neutral condition by Fackrell and Robins (1982). Profiles at four observation points in streamwise direction are shown, and each concentration is normalized by the maximum value of concentration at each profile of neutral condition. Mean concentration in neutral boundary layer corresponds with experimental data. Spreading widths of dispersion estimated by LES and experiment show quite well agreement.

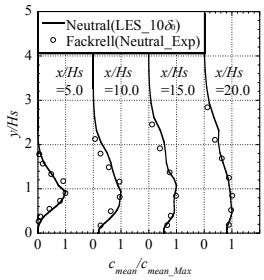

Figure 5: Time-averaged concentration in neutral TBL.

Rms concentration. Figure 6 shows vertical profiles of rms concentration for a plume dispersion emitted from an elevated point source in neutral turbulent boundary layer. Rms concentrations estimated by LES are a little unstable because of insufficient statistical data, but almost in good agreement with experimental data obtained by Fackrell and Robins(1982).

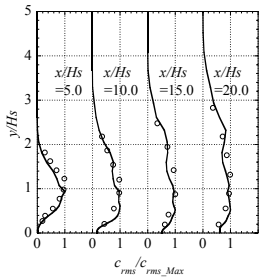

Figure 6: Concentration fluctuations in neutral TBL.

Stable Boundary Layer

Figures 7 and 8 show the dependency of the time-averaged concentration and concentration fluctuation on thermal stability of turbulent boundary layers. Time-averaged concentration spreads narrower and its peak values in the plume axis become much larger as the thermal stability increases. Even in the case of weak stable condition the value of concentration is approximately double along the center of plume. Concentration fluctuations also show same tendencies as the stability increases.

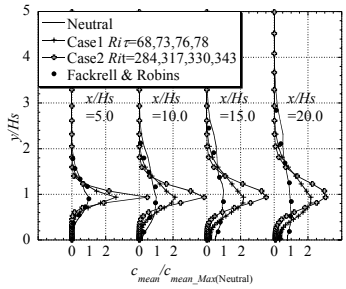

Figure 7: Time-averaged concentration in stable TBL.

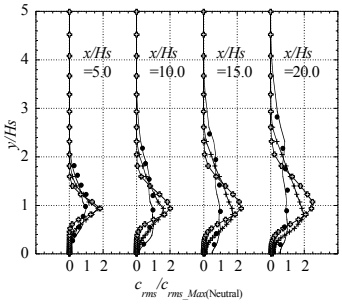

Figure 8: Concentration fluctuations in stable TBL.

Pasquill-Gifford diagrams. The data shown in figure 7 are plotted on the Pasquill-Gifford diagrams in figure 9. LES results indicate both of weak and strong stabilities. So, this means LES results are mechanically reasonable as behaviour of a plume dispersion.

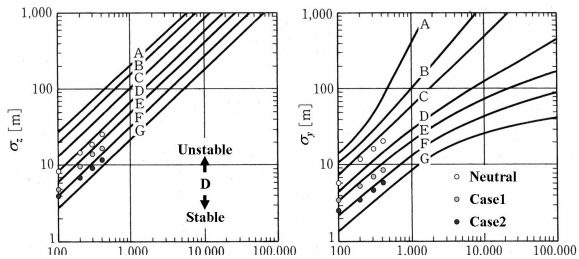

Figure 9: Plots on Pasquill-Gifford diagrams.

COMPUTATIONAL RESULTS FOR ATMOSPHERIC BOUNDARY LAYERS

As shown in figure 10(Stull, 1988), a nocturn stable boundary layer has various types of temperature profiles for time during night. In figure 11 Mahrt (1998) shows various types of temperature profiles with an inversion layer which is located at top of boundary layer after sunset (capping inversion) or near ground before sunrise (surface inversion). We set up three types of turbulent boundary layers as computational examples, which consist of the neutral TBL, the weakly stable TBL with a linear temperature profile and the strongly stable TBL with a polynomial temperature profile. Figure 12 represents these temperature profiles for a linear or a polynomial type.

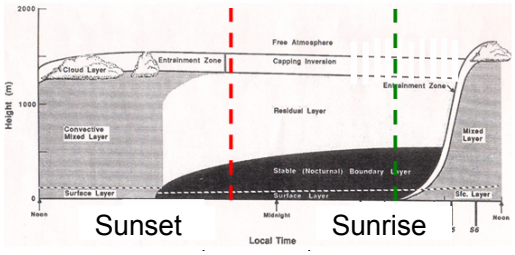

Figure 10: Diurnal cycle of atmospheric turbulent boundary layer (Stull, 1988).

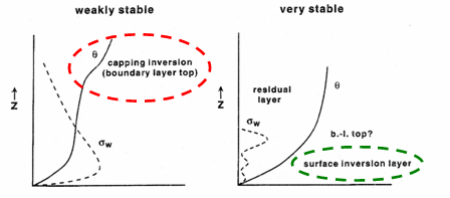

Figure 11: Various types of temperature profiles with an inversion layer (Mahrt, 1998).

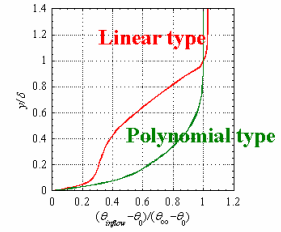

Figure 12: Linear and polynomial types of temperature profiles.

Turbulence Characteristics of Stable Boundary Layer

As shown in figures 13 ans 14, streamwise and vertical velocity fluctuations of linear type decrease in capping inversion layer with the stability rising such as experimental data obtained by Ohya and Uchida (2003). In figures 16 and 17, streamwise and vertical velocity fluctuations of polynomial type decrease in surface inversion layer with the stability rising such as experimental data(Ohya et al., 1997). In the case of neutral condition, we perform comparison of streamwise velocity with wind tunnel experiments by DeGraaff and Eaton(2000). The present LES results are consistent with DeGraaff's experimental data. Figures 15 and 18 show the mean temperature profiles of linear and polynomial types. Both of top and surface inversion layers in the stable turbulent boundary layer are definitely simulated well.

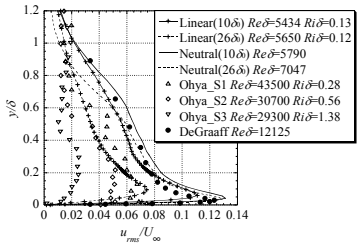

Figure 13: streamwise velocity fluctuation(Linear type).

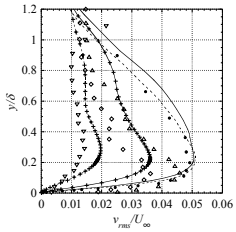

Figure 14: vertical velocity fluctuation(Linear type).

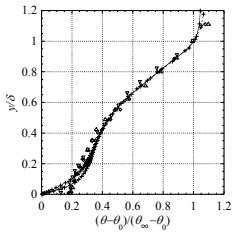

Figure 15: Mean temperature(Linear type).

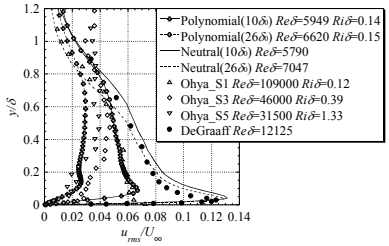

Figure 16: streamwise velocity fluctuation(Polynomial).

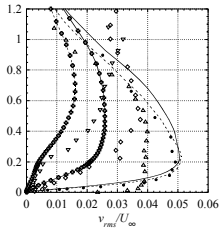

Figure 17: vertical velocity fluctuation(Polynomial type).

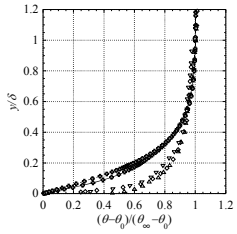

Figure 18: Mean temperature(Polynomial type).

Concentration Characteristics in Stable Boundary Layer

We analyze the behaviour of the dispersion plumes emitted from an elevated source point (x=10δ_0, y=0.2δ_0). Figure 19 depicts typical snapshots of the plume in the vertical section under neutral and stable conditions. Two iso-surfaces indicate 1% and 0.1% of emit intensity. Dispersion in stable boundary layer with a linear and a polynomial types of temperature profiles is more suppressed than in neutral boundary layer. A large plume meandering is frequently seen in neutral boundary layer, but the range of meandering seems to be narrow in stable cases. In the case of linear type, there is a top inversion which avoids the plume to acsend. Also, with regard to the averaged location of reattachment on the ground, the stable cases show farther position from the source point than the neutral case. Especially the polynomial type confines the plume at the same height and reduces the concentration fluctuation very much because the surface inversion exists near the ground and suppresses the near-wall fluid motions which play a key role for generation of turbulence.

Figures 20 and 21 show the vertical profiles of mean concentration and concentration fluctuation. Stable cases have a narrower spreading width and a higher concentration than neutral case. A polynomial type is more stable with small turbulence, so has a narrower width and a higher concentration. The characteristics of concentration fluctuation are consistent with the mean concentration results.

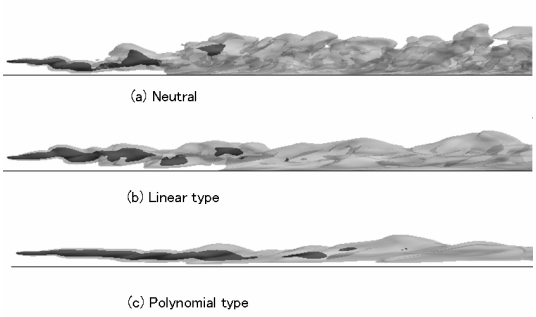

Figure 19: Instantaneous concentration fields in vertical section.

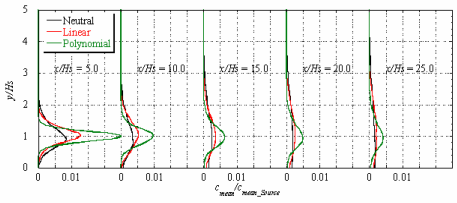

Figure 20: mean concentration profiles.

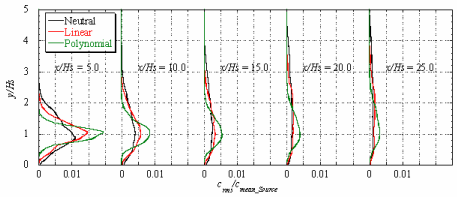

Figure 21: Concentration fluctuation profiles.

Statistical Estimation of Peak Concentration

Figure 22 shows time variations of concentration. Higher peaks are frequently observed in the case of stronger stable case. According to the probability distribution functions in figure 23, stronger stable case tends to indicate the clipping normal distribution which shows a convex curve upward.

Figure 24 shows streamwise variations of 90% peak factor. Peak factor has a larger value with approaching the source point. In the far region, the peak value is convergent to 3.0 for all cases. In stable conditions, the rms values of concentration are generally large, so the peak factors tend to become small.

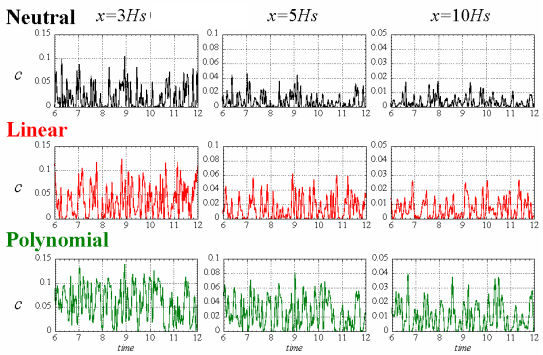

Figure 22: Time variations of concentrations.

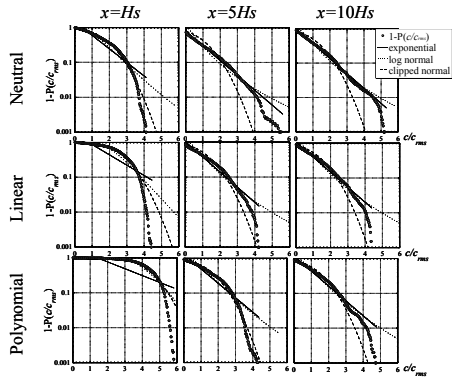

Figure 23: Probability distribution functions of concentrations.

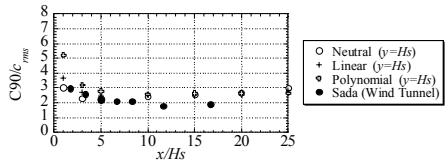

Figure 24: Streamwise variations of instantaneous peak factor of concentration.

CONCLUSIONS

This paper investigates the dispersion characteristics of plumes emitted from an elevated source point in spatially-developing thermally stratified turbulent boundary layer, including concentration fluctuations and their peak values. Conclusions are as follows:

In comparison with the previous experimental data, appropriate estimation of inflow turbulence causes good LES results.

Concentration characteristics in various types of atmospheric stable turbulent boundary layers with inversion layer are investigated, the inversion layer largely affects dispersion behaviour.

The present computational results indicate the statistical estimation of concentrations such as the probability distribution function or the occurrence of the peak values is possible by using the time-sequential data obtained by the LES models.

REFERENCES

Armerio, V. and Sarkar, S., 2002,'An investigation of stably stratified turbulent channel flow using large-eddy simulation', J. Fluid Mech., vol. 459, pp. 1-42.

DeGraaff, D.B. and Eaton, J.K., 2000,'Reynolds-number scaling of the flat-plate turbulent boundary layer', J. Fluid Mech., vol. 422, pp. 319-346.

Fackrell, J.E. and Robins, A.G., 1982,'Concetration fluctuations and fluxes in plumes from point sources in a turbulent boundary layer', J Fluid Mech., vol. 117, pp. 1-26.

Henn, D.S. and Sykes, R.I., 1992,'Large-eddy simulation of dispersion in the convective boundary layer', Atmos. Environ., vol. 26A, pp. 3145-3159.

Lund, T.S., Wu, X. and Squire, K.D., 1998,'Generation of turbulent inflow data for spatially developing boundary layer simulation', J. Comput. Phys., vol. 140, pp. 233-258.

Mahrt, L., 1998,' Stratified atmospheric boundary layers and breakdown of models', Comput. Fluid Dynamics, Vol. 11, pp. 263-279

Mason, P.J., 1992,'Large-eddy simulation of dispersion in convective bounday layers with wind shear', Atmos. Environ., vol. 26A, pp. 1561-1571.

Ohya, Y., Neff, D. E. And Meroney, R. N., 1997,' Turbulence structure in a stratified boundary layer under stable conditions', Boundary-layer Meteorology, Vol. 83, pp. 139-161.

Ohya, Y. and Uchida, T, 2003,' Turbulence structure of stable boundary layers with a near-linear temperature profile', Boundary-layer Meteorology, Vol. 108, pp. 19-38.

Stull, R. B., 1988,'An Introduction to boundary-layer meteorology', Kluwer Academic Publishers.

Sykes, R.I. and Henn, D.S., 1992,'Large-eddy simulation of concentration fluctuation in a dispering plume', Atmos. Environ., vol. 26A, pp. 3127-3144.

Tamura, T. et al., 2003,'LES analysis on dispersion in surface layer over randomly arranged roughness blocks', TSFP-3, vol.1, pp. 353-358.

Tamura, T. and Mori, K, 2006,'LES of spatially-developing stably stratified turbulent boundary layers', Direct and Large-Eddy Simulation VI, pp. 583-590.